

# Behavior Estimation from Multi-Source Data for Offline Reinforcement Learning

Guoxi Zhang<sup>1</sup> and Hisashi Kashima<sup>1,2</sup>

<sup>1</sup> Graduate School of Informatics, Kyoto University

<sup>2</sup> RIKEN Guardian Robot Project

guoxi@ml.ist.i.kyoto-u.ac.jp, kashima@i.kyoto-u.ac.jp

## Abstract

Offline reinforcement learning (RL) have received rising interest due to its appealing data efficiency. The present study addresses behavior estimation, a task that lays the foundation of many offline RL algorithms. Behavior estimation aims at estimating the policy with which training data are generated. In particular, this work considers a scenario where the data are collected from multiple sources. In this case, neglecting data heterogeneity, existing approaches for behavior estimation suffers from behavior misspecification. To overcome this drawback, the present study proposes a latent variable model to infer a set of policies from data, which allows an agent to use as behavior policy the policy that best describes a particular trajectory. This model provides with a agent fine-grained characterization for multi-source data and helps it overcome behavior misspecification. This work also proposes a learning algorithm for this model and illustrates its practical usage via extending an existing offline RL algorithm. Lastly, with extensive evaluation this work confirms the existence of behavior misspecification and the efficacy of the proposed model.

## 1 Introduction

Offline reinforcement learning (RL) (Lange, Gabel, and Riedmiller 2012) serves as a data-efficient RL setting in applications such as recommender systems (Chen et al. 2019) and robot manipulation (Dasari et al. 2020). In this setting, an agent learns policies using existing data that are assumed to be generated by an unknown policy called the behavior policy. An estimate of the behavior policy is an essential component of many offline RL algorithms, including the discounted COP-TD algorithm (Gelada and Bellemare 2019), the OPPOSD algorithm (Liu et al. 2020) and the BRAC-v algorithm (Wu, Tucker, and Nachum 2019).

The present study addresses behavior estimation—the task of estimating the behavior policy from data—in scenarios where data are collected from multiple sources. Typical scenarios include crowdsourcing demonstrations for robot manipulation (Mandlekar et al. 2018, 2021). Because different sources may prefer different actions, the action distributions can be multi-modal. Figure 1 shows a concrete example, where the green robot learns from data generated by two demonstrators. The blue demonstrator prefers to pass the

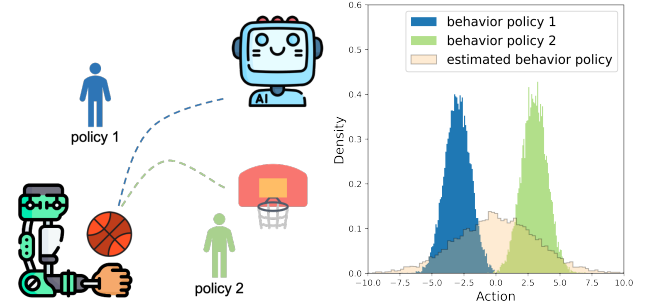


Figure 1: Example of multi-source trajectories (left) and behavior misspecification (right). The green robot learns to play basketball using data collected from the blue and green demonstrators. The blue demonstrator prefers to pass the ball to the other agent (policy 1), while the green demonstrator prefers to shoot (policy 2). A single estimate for the behavior policy will place probability mass at regions not covered by data.

ball to another agent, while the green demonstrator prefers to shoot. The empirical action distribution has two modes for that state, which leads to an issue called behavior misspecification. Consider the canonical approach for behavior estimation that assumes a single Gaussian policy for continuous problems. The histogram in orange in Figure 1 illustrates the action distribution induced by such a policy. Clearly, this distribution fails to model the underlying data.

Perhaps surprisingly, this canonical approach is widely adopted in literature (Gelada and Bellemare 2019; Liu et al. 2020; Pavse et al. 2020), and data heterogeneity has not receive much attention. While learning latent action spaces using variational autoencoder (VAE) (Kingma and Welling 2014) seems to be a remedy (Fujimoto, Meger, and Precup 2019; Zhou, Bajracharya, and Held 2020), the assumption of Gaussian action prior limits its expressiveness in multi-source scenarios.

The present study claims that, although the empirical action distribution is multi-modal, each individual data source still induces uni-modal action distributions. Thus, learning a set of behavior policies inducing uni-modal action distributions can successfully characterize data heterogeneity. In policy learning, this approach provides agents with the

most probable policy for specific trajectories through posterior inference. In the example shown in Figure 1, this corresponds to provide the agent with the fitted policy for the corresponding demonstrator when learning from some trajectory. Therefore, this approach provides agents with a better specification of the behavior policy compared to the canonical approach. To demonstrate this, this work proposes localized BRAC-v, which integrates this approach into the BRAC-v algorithm. BRAC-v demonstrates reasonable performance on single-source data but degenerate on multi-source data (Fu et al. 2020), so LBRAC-v showcases the efficacy of the proposed approach.

There are two remaining questions: how to estimate parameters of the behavior set and how to look up behavior policies for trajectories. This study addresses these questions with an embedding-based parameterization and a vector-quantized variational inference algorithm. The model embeds policies and trajectories into a low-dimensional space and learns these representation vectors by encouraging action reconstruction. After model learning, agents can use these embeddings to retrieve the corresponding policies for trajectories.

Finally, this study validates its claims empirically using the D4RL benchmark (Fu et al. 2020) and 15 new datasets. Algorithms that assume single behavior policy worsen on multi-source data, which confirms the detrimental effect of behavior misspecification. By contrast, LBRAC-v and existing VAE-based approaches achieve satisfactory performance on multi-source data. Further analysis shows that LBRAC-v outperforms existing VAE-based approaches on datasets of moderate size and quality, while the existing approaches are better on large high-quality datasets. These results illustrate the benefits and limitations of LBRAC-v. Lastly, visualizations indicate that the proposed model discovers patterns that are correlated with reward signals for trajectories, which are further polished in policy learning. Increasing the size of the behavior set encourages clustering trajectories with behavior policies but inhibits such reward-related patterns. The contributions of this work are summarized as follows.

- This work considers behavior estimation on multi-source data and highlights the detrimental effect of behavior misspecification.
- It proposes a latent variable model to learn a behavior set to overcome behavior misspecification. In addition, it proposes LBRAC-v to showcase how the model benefits policy learning.
- It demonstrates the efficacy of LBRAC-v with experiments and provides visualization-based explanations.

## 2 Related Work

Prior art for offline RL discusses issues such as value overestimation (Kumar et al. 2020) and poor convergence quality (Gelada and Bellemare 2019). Many require behavior estimation. For example, a line of work uses the behavior policy to compute the weights for importance sampling (Hallak and Mannor 2017; Gelada and Bellemare 2019; Nachum et al. 2019). Another active research direction introduces penalties for deviations against the behavior policy (Kumar

et al. 2019; Wu, Tucker, and Nachum 2019; Kostrikov et al. 2021). However, none of them considers if data are from multiple sources.

Meanwhile, it is worth mentioning the difference between this study and imitation learning from noisy demonstrations (Wu et al. 2019; Tangkaratt et al. 2020; Wang et al. 2021). Although the latter opts for a well-performing policy, such a policy does not necessarily reproduce the data accurately. In consequence, quantities such as importance weights will be biased when computed using the policy.

Although several offline RL algorithms learn latent action spaces using VAE (Fujimoto, Meger, and Precup 2019; Zhou, Bajracharya, and Held 2020; Zhang et al. 2022), their assumption of Gaussian priors can be problematic. By contrast, the proposed model learns a discrete set of behavior policies that address multiple modality in data.

## 3 Problem Statement

### Preliminaries

**Markov Decision Process:** An infinite-horizon discounted Markov decision process (MDP)  $\langle \mathcal{S}, \mathcal{A}, \mathcal{R}, P, \gamma \rangle$  is a mathematical model for decision-making tasks. A state  $s \in \mathcal{S}$  represents information provided to the agent for making a decision, and  $\mathcal{S}$  is the set of all possible states. An action  $a \in \mathcal{A}$  is an available option for a decision, and  $\mathcal{A}$  is the set of available actions. This study focuses on continuous control tasks, so actions are vectors in  $\mathbb{R}^{d_A}$ , where  $d_A \in \mathbb{N}_+$ . The reward function  $R : \mathcal{S} \times \mathcal{A} \rightarrow \mathbb{R}$  provides the agent with scalar feedback for each decision.  $P$  is a distribution over states conditioned on states and actions, which governs state transitions.  $\gamma \in (0, 1)$  is a hyperparameter known as the discount factor.

**Trajectories:** An MDP prescribes a sequential interaction procedure. Suppose the agent learns to navigate through a maze. Its current location is its state  $s \in \mathcal{S}$ . It selects  $a \in \mathcal{A}$  as the direction to go. Then, it is informed with its next state (next location)  $s' \sim P(s|s, a)$  and reward  $r = R(s, a)$ . For example,  $r = -1$  if the agent hits a wall, and  $r = 1$  if it reaches the target location. A trajectory is a sequence of states, actions and rewards. The  $m^{\text{th}}$  trajectory can be written as  $\tau_m = (s_{m,1}, a_{m,1}, r_{m,1}, s_{m,2}, a_{m,2}, r_{m,2}, \dots)$ , where the first and the second subscripts denote trajectory index and step index, respectively. In practice, trajectories are truncated to a finite length. The quality of  $\tau_m$  is measured by its sum of discounted rewards  $j(\tau_m) = \sum_{t=1}^{\infty} \gamma^{t-1} r_{m,t}$ . A useful notion is transition. A transition from  $\tau_m$  can be written as  $(s_m, a_m, r_m, s'_m)$ , which refers to two consecutive states, an action, and the corresponding reward for taking  $a_m$  at  $s_m$ .

**Policies and Q-functions:** An agent selects actions with a policy  $\pi : \mathcal{S} \rightarrow \Delta(\mathcal{A})$ , where  $\Delta(\mathcal{A})$  means the set of distributions over  $\mathcal{A}$ . This means that at  $s \in \mathcal{S}$ , it samples  $a$  from  $\pi(a|s)$ . The Q-function of  $\pi$ ,  $Q^\pi(s, a) : \mathcal{S} \times \mathcal{A} \rightarrow \mathbb{R}$ , gives the expected sum of discounted rewards obtained by taking  $a \in \mathcal{A}$  at  $s \in \mathcal{S}$  and subsequently following  $\pi$ . That is,  $Q^\pi(s) = \mathbb{E}_{\tau_m} [j(\tau_m) | s_{m,1} = s, a_{m,1} = a, \pi]$ .  $\pi$  is included in this expression to emphasize that it governs action selection at  $t > 1$ . The objective of policy learning is to compute

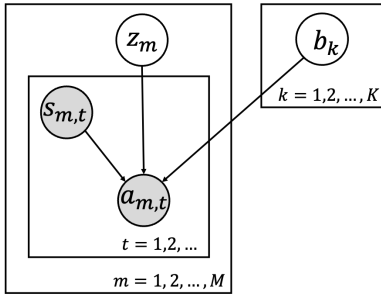


Figure 2: Graphical model representation for the proposed model.  $m$  is the index of trajectories, and  $t$  is the step index for states and actions in trajectories.  $\{b_k\}_{k=1}^K$  is a set of  $K$  behavior policies. To generate trajectory  $\tau_m$ , first sample a categorical variable  $z_m$  supported on  $\{1, 2, \dots, K\}$ . Then sample actions  $a_{m,t}$  from  $b_{z_m}(a|s_{m,t})$  once states  $s_{m,t}$  are observed.

a policy  $\pi^*$  such that  $Q^{\pi^*}(s, a) \geq Q^\pi(s, a), \forall s, a \in \mathcal{S} \times \mathcal{A}$ .

### Behavior Estimation from Multi-source Data

The input for behavior estimation is a fixed set of trajectories  $\mathcal{D} = \{\tau_m\}_{m=1}^M$ . Canonically,  $\mathcal{D}$  is assumed to be generated by a single policy  $b$  called the behavior policy. By contrast, this study considers  $\mathcal{D} = \{\tau_m\}_{m=1}^M$  to be generated by multiple policies from multiple sources. To this end, a learner is provided with access to the index of trajectories. For the sake of simplicity, this index is only referenced in subscripts.

The output is a behavior set  $\mathcal{B} = \{b_k\}_{k=1}^K$ , where  $b_k \in \mathcal{B}$  is a policy and  $K \in \mathbb{N}_+$  is the number of policies. Besides, the learner also outputs an assignment matrix  $G \in \{0, 1\}^{M \times K}$  of trajectories to  $\mathcal{B}$ , which enables it to use  $\mathcal{B}$  for policy learning.  $G_{u,v} = 1$  means that  $\tau_u$  is considered to be generated by  $b_v$ , and  $G_{u,v} = 0$  otherwise.  $G$  allows for retrieving the corresponding  $b_k \in \mathcal{B}$  for a given trajectory.

The learning problem can be summarized as follows.

- Input: offline trajectories  $\mathcal{D}$ .
- Output:  $K$  behavioral policies  $\mathcal{B} = \{b_k\}_{k=1}^K$  and the assignment matrix  $G$ .

## 4 Learning the Behavior Set

This section first describes the proposed model and its parameterization. Then it describes how parameters are estimated and the proposed LBRAC-v algorithm as a showcase for its usage.

### Proposed Latent-Variable Model

The proposed model assumes the following generative process. There are  $K$  different policies that may generate trajectories. To generate  $\tau_m$ , first sample a categorical variable  $z_m$  supported on  $\{1, 2, \dots, K\}$  and then roll out  $b_{z_m}$ . This means that, at step  $t$ , sample  $a_{m,t}$  from  $b_{z_m}(a|s_{m,t})$ . Figure 2 shows a graphical model representation of this process.

A running assumption is that each trajectory is generated solely by one policy in  $\mathcal{B}$ . Accordingly, the proposed model exploits the identity of trajectories when learning  $\mathcal{B}$ . To understand the benefit, consider two transitions

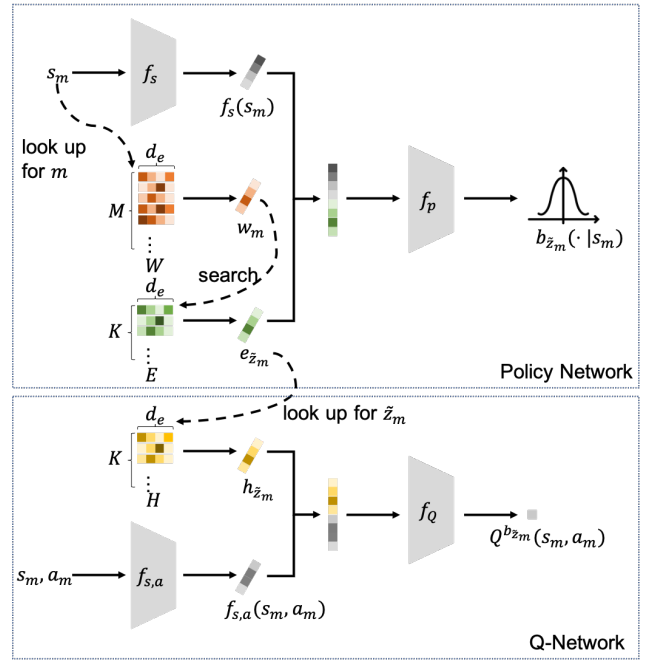


Figure 3: A diagram for the parameterization of the proposed model. Given  $(s_m, a_m)$ , the model looks up the  $m^{\text{th}}$  vector in  $W$  and uses it to search for  $e_{z_m}$  in  $E$ . See Equation 3 for details of searching.  $e_{z_m}$  is concatenated with vector  $f_\phi(s_m)$  and passed to  $f_\theta$  to generate actions. Meanwhile, the model looks up the  $z_m^{\text{th}}$  vector in  $H$  and concatenates it with  $g_\phi(s_m, a_m)$ . The concatenated vector is passed to  $g_\theta$  to compute Q values.

$(s_m, a_m, r_m, s'_m)$  and  $(s_{m'}, a_{m'}, r_{m'}, s'_{m'})$ , such that  $s_m = s_{m'}$ ,  $m \neq m'$ , and  $a_m \neq a_{m'}$ . When the two policies that generate  $\tau_m$  and  $\tau_{m'}$  differ, the existing VAE-based approaches becomes deficient, as they assume a Gaussian prior for actions. However, by assigning  $\tau_m$  and  $\tau_{m'}$  to different elements in  $\mathcal{B}$ , the proposed model can leverage the simplicity of Gaussian policies without sacrificing the flexibility for multi-source trajectories.

As illustrated in Figure 3, the proposed model consists of two major components: a policy network and a Q-network. The policy network represents  $\mathcal{B}$  using an embedding matrix  $E \in \mathbb{R}^{K \times d_e}$  and two functions  $f_s$ , and  $f_p$ , where  $d_e \in \mathbb{N}_+$ . Each row of  $E$  is an embedding vector for a policy in  $\mathcal{B}$ .  $f_s : \mathcal{S} \rightarrow \mathbb{R}^{d_\phi}$  is a function that computes state representations, where  $d_\phi \in \mathbb{N}_+$ .  $f_p : \mathbb{R}^{d_e} \times \mathbb{R}^{d_\phi} \rightarrow \mathbb{R}^{2 \times d_A}$  is a function that converts representations of states and policies to action distributions. For a state  $s_m$ , let  $\mu_{s_m}$  and  $\sigma_{s_m}$  be the mean and diagonal elements of the covariance matrix for the action distribution at  $s_m$ , respectively. Then,

$$[\mu_{s_m}^\top \sigma_{s_m}^\top] = f_p(e_{z_m}, f_s(s_m)). \quad (1)$$

In other words,  $f_p$  outputs the concatenation of mean vector and diagonal elements in the covariance matrix of the induced action distribution.

The Q-network of the proposed model uses an embedding matrix  $H \in \mathbb{R}^{K \times d_e}$  and two functions  $f_{s,a}$  and  $f_Q$ ,

to represent Q-functions of policies in  $\mathcal{B}$ . Each row in  $H$  is an embedding vector for the Q-function of a policy in  $\mathcal{B}$ .  $f_{s,a} : \mathcal{S} \times \mathcal{A} \rightarrow \mathbb{R}^{d'_\phi}$  encodes state and actions into vectors in  $\mathbb{R}^{d'_\phi}$ , where  $d'_\phi \in \mathbb{N}_+$ .  $g_\theta : \mathbb{R}^{d'_\phi + d_e} \rightarrow \mathbb{R}$  converts representations into Q-values:

$$Q^{b_z} = f_Q(h_z, f_{s,a}(s, a)). \quad (2)$$

Note that in both the policy network and the Q-network, all policies (or Q-functions) share  $f_s$  and  $f_p$  (or  $f_{s,a}$  and  $f_Q$ ), which reduces computational costs when compared to using  $K$  separate policy networks (or Q functions). Moreover, this parameter-sharing mechanism forces these functions to encode information that is common for all policies in  $\mathcal{B}$  (or their Q functions), which in turn improves their performance for representing  $\pi$ .

### Parameter Estimation

Parameters to be learned are  $E$ ,  $H$ , and neural networks for functions  $f_s$ ,  $f_p$ ,  $g_{s,a}$  and  $g_Q$ . Figure 3 depicts key operations of the learning algorithm. The main idea is to learn a matrix  $W \in \mathbb{R}^{M \times d_e}$  as variational parameters. Each row of this matrix is a embedding vector for a trajectory in  $\mathcal{D}$ . The proposed algorithm uses the following posterior distribution  $q(z_m | s_m, a_m)$ :

$$q(z_m = k | s_m, a_m) = \begin{cases} 1 & \text{for } k = \arg\max_j e_j w_m, \\ 0 & \text{otherwise.} \end{cases} \quad (3)$$

Let  $\tilde{z}_m = \arg\max_j e_j w_m$ . This posterior distribution places all probability mass on  $\tilde{z}_m$ , and  $e_{\tilde{z}_m}$  can be considered as the latent encoding for the behavior policy of  $\tau_m$ .

Overall, parameters are learned via action reconstruction. Assuming a uniform prior for  $z_m$ , this in turn maximizes the evidence lowerbound for actions. However, care must be taken, as what relates  $s_m$  and  $a_m$  to  $e_{\tilde{z}_m}$  in Equation 3 is a searching operation. There is no real gradient directly defined for  $w_m$ .

Inspired by the SOM-VAE (Fortuin et al. 2019), the proposed algorithm uses an objective consists of three terms:  $L_{\text{rec}}$ ,  $L_{\text{com}}$ , and  $L_Q$ . Specifically,  $L_{\text{rec}}$  encourages action reconstruction. Recall that  $f_p$  outputs parameters of action distributions, and let  $\ell$  be the log-likelihood function of the action distribution.

$$L_{\text{rec}} = -\ell(f_p(f_s(s_m), e_{\tilde{z}_m}); a_m) - \ell(f_p(f_s(s_m), w_m); a_m) \quad (4)$$

The first term encourages  $e_{\tilde{z}_m}$  to reconstruct actions, and the second term does likewise for  $w_m$ . Yet using Equation 4 alone,  $w_m$  is not related to  $e_{\tilde{z}_m}$ , so  $w_m$  and  $e_{\tilde{z}_m}$  are not updated in a way that is consistent with  $\tilde{z}_m = \arg\max_j e_j w_m$ .  $L_{\text{com}}$  mitigates this issue by penalizing the discrepancy between them:

$$L_{\text{com}} = 1 - w_m^\top e_{\tilde{z}_m}. \quad (5)$$

$L_Q$  is used for learning the Q-functions, which originates from fitted Q evaluation (Le, Voloshin, and Yue 2019).

$$L_Q = \mathbb{E}_{a' \sim b_{\tilde{z}_m}} (r_m + \gamma \bar{Q}^{b_{\tilde{z}_m}}(s_m, a') - Q^{b_{\tilde{z}_m}}(s_m, a_m))^2, \quad (6)$$

$\bar{Q}^{b_{\tilde{z}_m}}$  is the target network for  $Q^{b_{\tilde{z}_m}}$ .

In summary, for a transition  $(s_m, a_m, r_m, s'_m)$ , the proposed algorithm utilizes the following objective function:

$$L = L_{\text{rec}} + \alpha L_{\text{com}} + L_Q, \quad (7)$$

where  $\alpha$  is a hyper-parameter fixed to 0.1 in experiments. After learning, the assignment matrix  $G$  can be computed using  $W$  and  $E$ . The column index of the only non-zero element in the  $m^{\text{th}}$  row of  $G$  is  $\tilde{z}_m$ . Additional details for the proposed model is provided in Appendix A.

### The Proposed LBRAC-v Algorithm

To demonstrate how the proposed model improves offline RL, this study presents LBRAC-v, an extension of the BRAC-v algorithm (Wu, Tucker, and Nachum 2019). To begin with, this subsection first reviews BRAC-v and explains why it suffers from behavior misspecification.

BRAC-v extends the actor-critic framework by penalizing the discrepancy between the policy being learned  $\pi$  and a single behavior policy  $b$ . On a transition, it minimizes the following objectives:

$$\begin{aligned} L_{\text{critic}} &= \mathbb{E}_{a' \sim \pi(\cdot | s'_m)} [r_m + \gamma(\bar{Q}^\pi(s'_m, a') - \beta D(\pi, b, s'_m)) \\ &\quad - Q^\pi(s_m, a_m)]^2, \\ L_{\text{actor}} &= \mathbb{E}_{a'' \sim \pi(\cdot | s_m)} [\beta D(\pi, b, s_m) - Q^\pi(s_m, a'')] . \end{aligned} \quad (8)$$

$\bar{Q}^\pi$  is the target network for  $Q^\pi$ .  $D(\pi, b, s)$  estimates the discrepancy between  $\pi(\cdot | s)$  and  $b(\cdot | s)$ , and  $\beta$  is a hyperparameter. Essentially, BRAC-v subtracts the Q value at  $s'_m$  (or  $s_m$ ) by  $\beta D(\pi, b, s'_m)$  (or  $\beta D(\pi, b, s_m)$ ) to penalize  $\pi$  for deviating from  $b$ . Wu, Tucker, and Nachum (2019) suggested using KL-divergence for  $D(\pi, b, s)$ :

$$D(\pi, b, s) = \mathbb{E}_{a \sim \pi(\cdot | s)} [\log(\pi(a | s)) - \log(b(a | s))] . \quad (9)$$

Because BRAC-v assumes a single behavior policy, it faces issues when handling multi-source data. Consider again the example in Figure 1. As the mode of the estimated single behavior policy locates between modes of the two behavior policies,  $D(\pi, b, s)$  unfortunately takes the minimum value between data modes. In consequence, BRAC-v encourages  $\pi$  to take out-of-distribution actions.

To overcome this drawback, LBRAC-v integrates the proposed model into BRAC-v. Essentially, when learning from  $\tau_m$ , it first find  $b_{\tilde{z}_m}$  in  $\mathcal{B}$  and then penalizes the deviation of  $\pi$  against  $b_{\tilde{z}_m}$ . In this way, LBRAC-v will not encourage  $\pi$  to take out-of-distribution actions.

Another idea behind LBRAC-v is to reuse  $f_s$ ,  $f_p$ ,  $f_{s,a}$ , and  $f_Q$  of a trained proposed model to represent  $\pi$  and  $Q^\pi$ . Because these functions are adapted to the entire behavior set, they are also suitable for policies that are close to  $\mathcal{B}$ . Thus, LBRAC-v can benefit from the parameter-sharing mechanism of the proposed model. Specifically, LBRAC-v learns two vectors  $e_\pi \in \mathbb{R}^{d_e}$  and  $h_\pi \in \mathbb{R}^{d_e}$  as embedding vectors for  $\pi$  and  $Q^\pi$ .  $\pi$  is parameterized by replacing  $e_{\tilde{z}_m}$  with  $e_\pi$  in Equation 1, and  $Q^\pi$  is parameterized by replacing  $h_z$  with  $h_\pi$  in Equation 2. In practice,  $e_\pi$  and  $h_\pi$  may be added



to a trained proposed model to jointly optimize Equation 8 and Equation 7.

As a final remark, the proposed model can be straightforwardly integrated with other offline algorithms that utilizes parametric estimates of the behavior policy or latent action spaces. The present study presents LBRAC-v to illustrate how practitioners can extend existing algorithms for multi-source datasets.

## 5 Experiments

### Datasets

This study uses three continuous control tasks in evaluation: halfcheetah, walker2d, and hopper. For each task, four versions of datasets were taken from the D4RL benchmark (Fu et al. 2020). The random and medium versions were generated by a random policy and an RL agent, respectively. The medium-replay version contains transitions collected for training the RL agent, and the medium-expert version is a combination of medium version with expert demonstrations. The former two are single-source datasets, whereas the latter two are multi-source datasets.

However, as shown in Table 3 in Appendix B, for the same task these datasets differ in two of the three aspects: the number of behavior policies, the number of transitions, and the quality of behavior policies. They cannot directly reveal how the number of behavior policies affects performance. Thus, this study generates five new datasets for each task, denoted as heterogeneous- $k$  ( $k \in \{1, 2, 3, 4, 5\}$ )<sup>1</sup>. For each task, first train five soft actor-critic (SAC) (Haarnoja et al. 2018) for an equal number of steps. Then, generate the heterogeneous- $k$  version by rolling out the first  $k$  agents for one million transitions. Each agent contributed to the same amount. Consequently, heterogeneous- $k$  only differ in the number of behavior policies, which allows for investigating data heterogeneity.

Statistics of all the datasets and more details for heterogeneous- $k$  are provided in Table 3 in Appendix B.

### Alternative Methods

Alternative methods are selected for three purposes. BC, BRAC-v and CQL, and MOPO are selected to demonstrate detrimental effect of behavior misspecification. MOPP and F-BRC are selected to show that latest algorithms with sophisticated parameterization for behavior policies still suffer from this issue. BCQ and PLAS are two existing VAE-based approaches. They are selected to investigate whether and when learning a behavior set is beneficial.

- BC: a method that uses an estimated single behavior policy as output.
- BRAC-v (Wu, Tucker, and Nachum 2019): a model-free method that minimizes the KL divergence against an estimated single behavior policy.
- CQL (Kumar et al. 2020): a model-free method that computes empirical expectations over actions in data.
- MOPO (Yu et al. 2020): a model-based algorithm that estimates state transition distributions.

- MOPP (Zhan, Zhu, and Xu 2022): a model-based algorithm that uses an ensemble of autoregressive dynamics models as the behavior policy.
- F-BRC (Kostrikov et al. 2021): a model-free method that minimizes the Fisher divergence against a mixture of behavior policies.
- BCQ (Fujimoto, Meger, and Precup 2019): an algorithm that learns a VAE for actions.
- PLAS (Zhou, Bajracharya, and Held 2020): an algorithm that learns a VAE for actions and uses it to represent  $\pi$ .

Results on the D4RL datasets for BC, BRAC-v, CQL, and BCQ are taken from (Fu et al. 2020), and results for F-BRC, MOPO, MOPP, and PLAS are taken from the corresponding papers. For heterogeneous- $k$  datasets, the present study used the code provided by Fu et al. (2020) for BRAC-v and BCQ and the official code for CQL and PLAS.

### Evaluation Metric

Algorithms are compared by trajectory returns (i.e. non-discounted sum of rewards) obtained over 20 test runs. Returns are normalized into 0-100 scale as suggested by Fu et al. (2020). The higher, the better. See Appendix B for more details.

Because of the inherent randomness of training RL agents, there is performance fluctuation among the behavior policies for heterogeneous- $k$ . To eliminate this fluctuation, for experiments on these datasets the present study uses the ratio between normalized returns of an algorithm and the average normalized returns of behavior policies as evaluation metric. This metric is termed *relative return*.

### Implementation Details

$d_e$  is set to eight.  $f_s$  and  $f_p$  are parameterized by two layers of feed-forward networks with 200 hidden units, while  $f_{s,a}$  and  $f_Q$  are parameterized similarly but with 300 hidden units. The learning rates for the policy network and the Q-network were  $5 \times 10^{-5}$  and  $1 \times 10^{-4}$ . Other details are available in Appendix A and the code is available here<sup>2</sup>.

The proposed model and LBRAC-v are trained for  $K \in \{1, 5, 10, 15, 20\}$ . Table 1 reports the best value for each dataset, and Table 4 and Table 5 reports results for all  $K$ . Experiments are repeated for five different random seeds, and this paper reports the average value of metrics and standard errors.

### Results

First, compare LBRAC-v with BRAC-v, CQL, and MOPO. As shown in Figure 4, performance of BRAC-v and CQL worsen on data generated by multiple policies. When  $k = 5$ , BRAC-v merely achieves less than 50% of its performance for  $k = 1$ . In contrast, LBRAC-v outperforms BRAC-v and achieves consistent performance for various value of  $k$ . Table 1 shows results on D4RL datasets. Although BRAC-v has intermediate performance on medium versions, it fails on the medium-replay version of walker2d and the medium-replay and medium-expert version of hopper. CQL has

<sup>1</sup><https://zenodo.org/record/7375417#.Y4Wzti9KGgQ>

<sup>2</sup>[https://github.com/Altriaex/multi\\_source\\_behavior\\_modeling](https://github.com/Altriaex/multi_source_behavior_modeling)

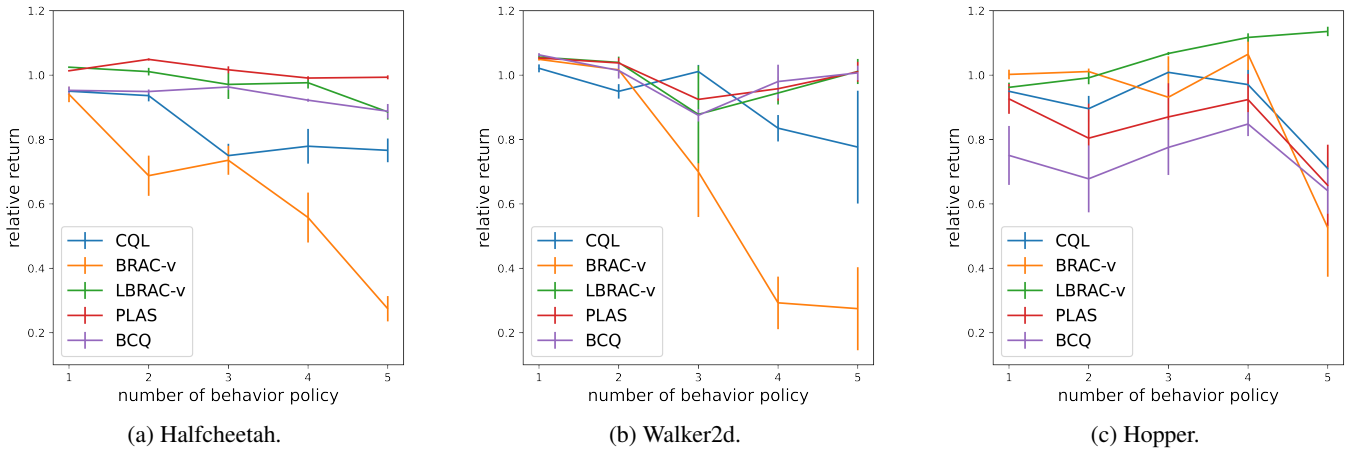


Figure 4: Results on heterogeneous- $k$  datasets. The performance of CQL and BRAC-v degenerates when data are generated by multiple behavior policies, which confirms the existence of behavior miss-specification. The proposed LBRAC-v overcomes such drawback of BRAC-v on multi-source data. VAE-based approaches are also robust on multi-source data.

Table 1: Results on D4RL datasets. The best method for each dataset is highlighted in bold. LBRAC-v outperforms BRAC-v on eight datasets and achieves the best performance on four datasets. Compared to VAE-based methods (PLAS and BCQ), LBRAC-v performs better on medium and medium-replay versions.

Task	Version	BC	F-BRC	MOPP	PLAS	BRAC-v	CQL	BCQ	MOPO	LBRAC-v
halfcheetah	random	2.1	33.3 $\pm$ 1.3	9.4 $\pm$ 2.6	25.8	31.2	<b>35.4</b>	2.2	<b>35.4<math>\pm</math>2.5</b>	26.37 $\pm$ 0.29
	medium	36.1	41.3 $\pm$ 0.3	44.7 $\pm$ 2.6	42.2	46.3	44.4	40.7	42.3 $\pm$ 1.6	<b>52.14<math>\pm</math>0.11</b>
	medium-replay	38.4	43.2 $\pm$ 1.5	43.1 $\pm$ 4.3	43.9	47.7	46.2	38.2	<b>53.1<math>\pm</math>2.0</b>	48.41 $\pm$ 0.14
	medium-expert	35.8	93.3 $\pm$ 10.2	106.2 $\pm$ 5.1	<b>96.6</b>	41.9	62.4	64.7	63.3 $\pm$ 38.8	94.22 $\pm$ 1.00
walker2d	random	2.1	1.5 $\pm$ 0.7	6.3 $\pm$ 0.1	3.1	1.9	7.0	4.9	<b>13.6<math>\pm</math>2.6</b>	11.96 $\pm$ 4.39
	medium	36.1	78.8 $\pm$ 1.0	80.7 $\pm$ 1.0	66.9	81.1	79.2	53.1	17.8 $\pm$ 19.3	<b>82.40<math>\pm</math>1.30</b>
	medium-replay	38.4	41.8 $\pm$ 7.9	18.5 $\pm$ 8.4	30.2	0.9	26.7	15.0	39.0 $\pm$ 9.6	<b>76.18<math>\pm</math>4.47</b>
	medium-expert	35.8	105.2 $\pm$ 3.9	92.9 $\pm$ 14.1	89.6	81.6	<b>111.0</b>	57.5	44.6 $\pm$ 12.9	109.65 $\pm$ 0.23
hopper	random	2.1	11.3 $\pm$ 0.2	<b>13.7<math>\pm</math>2.5</b>	10.5	12.2	10.8	10.6	11.7 $\pm$ 0.4	9.63 $\pm$ 0.27
	medium	36.1	99.4 $\pm$ 0.3	31.8 $\pm$ 1.3	36.9	31.1	58.0	54.5	28.0 $\pm$ 12.4	<b>100.50<math>\pm</math>0.57</b>
	medium-replay	38.4	35.6 $\pm$ 1.0	32.3 $\pm$ 5.9	27.9	0.6	48.6	33.1	67.5 $\pm$ 24.7	<b>81.89<math>\pm</math>12.77</b>
	medium-expert	35.8	<b>112.4<math>\pm</math>0.3</b>	95.4 $\pm$ 28	111.0	0.8	98.7	110.9	23.7 $\pm$ 6.0	98.08 $\pm$ 6.39

strong performance on medium-expert versions but not on medium-replay versions. In contrast, LBRAC-v surpasses BRAC-v on 10 datasets and CQL on nine datasets. It also outperforms MOPO on medium versions and both multi-source versions, except for the medium-replay version of halfcheetah. These results confirm the existence of behavior miss-specification and the efficacy of LBRAC-v on both multi-source and single-source data.

Then compare LBRAC-v with F-BRC and MOPP. While they use sophisticated parameterization for behavior policies, they still overlook potential issues of multi-source datasets. Figure 4 shows LBRAC-v outperforms F-BRC on nine of the twelve datasets and MOPP on ten of the twelve datasets. These results corroborate the importance of considering behavior misspecification

Now compare LBRAC-v with PLAS and BCQ, the two VAE-based algorithms. As shown in Figure 4, LBRAC-v outperforms BCQ and PLAS on the heterogeneous- $k$  versions for hopper, but it was outperformed by PLAS for

halfcheetah. For walker2d, the three methods had similar performance. These results indicate that both the VAE-based approach and the proposed model can model multi-source data. Table 1 reveals the strength and weakness of these two lines of approaches. LBRAC-v outperforms PLAS on all the medium and medium-replay versions and the random version for halfcheetah and walker2d. It outperforms BCQ on every datasets except for the random and medium-expert versions of hopper. In short, PLAS and BCQ have better performance on the medium-expert versions but not for the rest. As shown in Table 3 in Appendix B, this version has one time more samples than other versions, and its average returns is also one time better. It concludes that the VAE-based approach is suitable for large and high-quality datasets, whereas the proposed model is suitable for small or low-quality datasets.

Finally, this study provides insights about the proposals using visualizations. They are created by projecting  $W$  to 2D space using principle component analysis and transform-

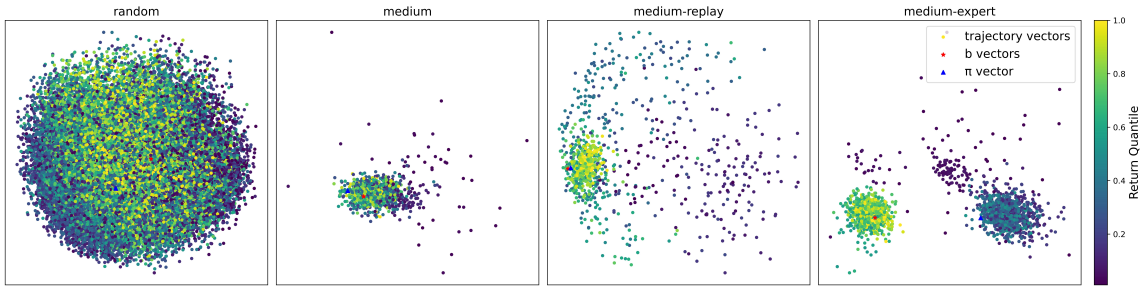


Figure 5: Visualizations of LBRAC-v on the four versions of walker2d datasets provided by D4RL.  $K = 1$ . Trajectories are clustered by returns, especially for medium-replay and medium-expert versions.

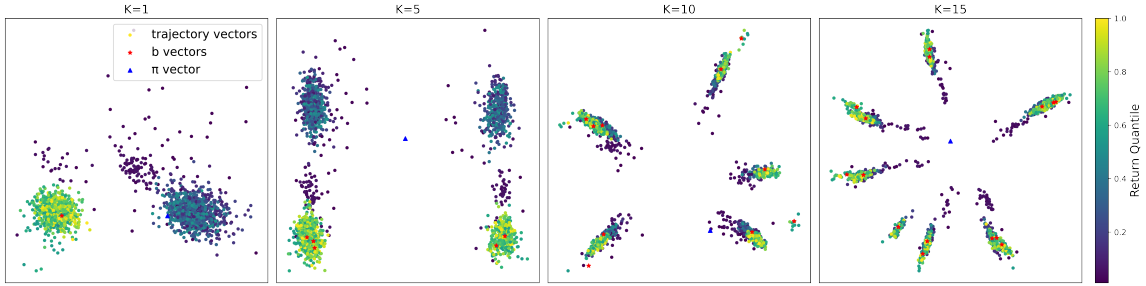


Figure 6: Visualizations of LBRAC-v on the medium-expert version of walker2d with different values of  $K$ . Increasing  $K$  results in fine-grained clustering of trajectories around behavior policies, but reward-related patterns become less apparent.

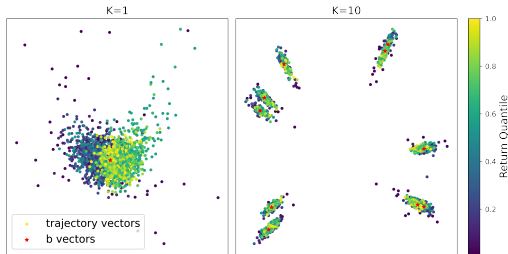


Figure 7: Visualizations of the proposed model on the medium-expert version of walker2d.

ing  $E$  and  $e_\pi$  to that space. Figure 5 shows visualizations of LBRAC-v for walker2d datasets.  $K$  is set to one to analyze effects of parts other than  $E$ . Trajectories are clustered by returns, which indicates that sharing  $w_m$  for actions in  $\tau_m$  facilitates discovering reward-related patterns. For reference, the left part of Figure 7 shows the visualization of the proposed model on medium-expert version of walker2d when  $K = 1$ . Reward-related patterns are also discovered, but they are less distinctive than those in Figure 5. This observation implies that during policy learning return-related patterns are polished with information from rewards.

Figure 6 shows visualizations for the case of various  $K$ . Increasing  $K$ , trajectory clusters are squeezed towards policy vectors, and reward-related patterns becomes less distinctive. The right part of Figure 7 reveals that it is the proposed model that fails to discover such patterns. Together, these visualizations suggest the followings.

1. For small  $K$ , the proposed model discovers reward-related patterns for trajectories.
2. Such patterns get polished in policy learning.
3. Large value of  $K$  encourages clustering trajectories by behavior policies but inhibits reward-related patterns.

Interested readers may find visualization obtained during training in Figure 9 in Appendix C for more insights.

## 6 Conclusion

Behavior estimation is a premise task of many offline RL algorithms. This work considers a scenario where training data are collected from multiple sources. This work identifies an issue called behavior misspecification in this scenario, which means the assumption of single behavior policy fails in this scenario. To address this issue, this work proposes a latent variable model to estimate a set of behavior policies from data and integrates this model to the BRAC-v algorithm to showcase its usage. Empirical results confirm the existence of behavior misspecification and demonstrate the efficacy of the proposed model and the proposed extension. Moreover, visualizations show that the proposed model discovers reward-related patterns for trajectories, which are further enhanced in policy learning. The present study is one of the few if any that addresses behavior estimation on multi-source data in literature and lays foundation for applying of-line RL in real-world applications.

## Acknowledgements

This work was supported by JST CREST Grant Number JP-MJCR21D1. The authors would like to thank Han Bao for

valuable feedback on an early draft of this paper.

## References

- Ba, J. L.; Kiros, J. R.; and Hinton, G. E. 2016. Layer Normalization. arXiv:1607.06450.
- Chen, M.; Beutel, A.; Covington, P.; Jain, S.; Belletti, F.; and Chi, E. H. 2019. Top-K Off-Policy Correction for a REINFORCE Recommender System. In *Proceedings of the Twelfth ACM International Conference on Web Search and Data Mining*, 456–464. Melbourne, Australia: ACM.
- Dasari, S.; Ebert, F.; Tian, S.; Nair, S.; Bucher, B.; Schmeckpeper, K.; Singh, S.; Levine, S.; and Finn, C. 2020. RoboNet: Large-Scale Multi-Robot Learning. In *Proceedings of the Third Conference on Robot Learning*, 885–897. Osaka, Japan: PMLR.
- Fortuin, V.; Hüser, M.; Locatello, F.; Strathmann, H.; and Rätsch, G. 2019. SOM-VAE: Interpretable Discrete Representation Learning on Time Series. In *Proceedings of the Seventh International Conference on Learning Representations*. New Orleans, LA, USA: OpenReview.net.
- Fu, J.; Kumar, A.; Nachum, O.; Tucker, G.; and Levine, S. 2020. D4RL: Datasets for Deep Data-Driven Reinforcement Learning. arXiv:2004.07219.
- Fujimoto, S.; Meger, D.; and Precup, D. 2019. Off-Policy Deep Reinforcement Learning without Exploration. In *Proceedings of the Thirty-Sixth International Conference on Machine Learning*, 2052–2062. Long Beach, CA, USA: PMLR.
- Gelada, C.; and Bellemare, M. G. 2019. Off-Policy Deep Reinforcement Learning by Bootstrapping the Covariate Shift. In *Proceedings of the Thirty-Third AAAI Conference on Artificial Intelligence*, 3647–3655. Honolulu, Hawaii, USA: AAAI Press.
- Haarnoja, T.; Zhou, A.; Abbeel, P.; and Levine, S. 2018. Soft Actor-Critic: Off-Policy Maximum Entropy Deep Reinforcement Learning with a Stochastic Actor. In *Proceedings of the Thirty-Fifth International Conference on Machine Learning*, 1861–1870. Stockholm, Sweden: PMLR.
- Hallak, A.; and Mannor, S. 2017. Consistent On-Line Off-Policy Evaluation. In *Proceedings of the Thirty-Fourth International Conference on Machine Learning*, 1372–1383. Sydney, Australia: PMLR.
- Kingma, D. P.; and Welling, M. 2014. Auto-Encoding Variational Bayes. In Bengio, Y.; and LeCun, Y., eds., *Proceedings of the Second International Conference on Learning Representations*. Banff, AB, Canada.
- Kostrikov, I.; Fergus, R.; Tompson, J.; and Nachum, O. 2021. Offline Reinforcement Learning with Fisher Divergence Critic Regularization. In *Proceedings of the Thirty-Eighth International Conference on Machine Learning*, 5774–5783. Virtual: PMLR.
- Kumar, A.; Fu, J.; Soh, M.; Tucker, G.; and Levine, S. 2019. Stabilizing Off-Policy Q-Learning via Bootstrapping Error Reduction. In *Advances in Neural Information Processing Systems*, volume 32, 11784–11794. Vancouver, BC, Canada: Curran Associates, Inc.
- Kumar, A.; Zhou, A.; Tucker, G.; and Levine, S. 2020. Conservative Q-Learning for Offline Reinforcement Learning. In *Advances in Neural Information Processing Systems*, volume 33, 1179–1191. Virtual: Curran Associates, Inc.
- Lange, S.; Gabel, T.; and Riedmiller, M. 2012. *Batch Reinforcement Learning*, 45–73. Springer Berlin Heidelberg.
- Le, H.; Voloshin, C.; and Yue, Y. 2019. Batch Policy Learning under Constraints. In *Proceedings of the Thirty-Sixth International Conference on Machine Learning*, 3703–3712. Long Beach, CA, USA: PMLR.
- Liu, Y.; Swaminathan, A.; Agarwal, A.; and Brunskill, E. 2020. Off-Policy Policy Gradient with Stationary Distribution Correction. In *Proceedings of the Thirty-Fifth Uncertainty in Artificial Intelligence Conference*, 1180–1190. Tel Aviv, Israel: PMLR.
- Mandlekar, A.; Xu, D.; Wong, J.; Nasiriany, S.; Wang, C.; Kulkarni, R.; Fei-Fei, L.; Savarese, S.; Zhu, Y.; and Martín-Martín, R. 2021. What Matters in Learning from Offline Human Demonstrations for Robot Manipulation. In *Proceedings of the Fifth Annual Conference on Robot Learning*. London, UK.
- Mandlekar, A.; Zhu, Y.; Garg, A.; Booher, J.; Spero, M.; Tung, A.; Gao, J.; Emmons, J.; Gupta, A.; Orbay, E.; Savarese, S.; and Fei-Fei, L. 2018. ROBOTURK: A Crowdsourcing Platform for Robotic Skill Learning through Imitation. In *Proceedings of the Second Conference on Robot Learning*, 879–893. Zürich, Switzerland.
- Nachum, O.; Chow, Y.; Dai, B.; and Li, L. 2019. DualDICE: Behavior-Agnostic Estimation of Discounted Stationary Distribution Corrections. In *Advances in Neural Information Processing Systems*, volume 32. Vancouver, Canada: Curran Associates, Inc.
- Pavse, B.; Durugkar, I.; Hanna, J.; and Stone, P. 2020. Reducing Sampling Error in Batch Temporal Difference Learning. In *Proceedings of the Thirty-Seventh International Conference on Machine Learning*, 7543–7552. Virtual.
- Tangkaratt, V.; Han, B.; Khan, M. E.; and Sugiyama, M. 2020. Variational Imitation Learning with Diverse-quality Demonstrations. In *Proceedings of the Thirty-Seventh International Conference on Machine Learning*, 9407–9417. Virtual: PMLR.
- Wang, Y.; Xu, C.; Du, B.; and Lee, H. 2021. Learning to Weight Imperfect Demonstrations. In *Proceedings of the Thirty-Eighth International Conference on Machine Learning*, 10961–10970. Virtual: PMLR.
- Wu, Y.; Tucker, G.; and Nachum, O. 2019. Behavior regularized offline reinforcement learning. arXiv:1911.11361.
- Wu, Y.-H.; Charoenphakdee, N.; Bao, H.; Tangkaratt, V.; and Sugiyama, M. 2019. Imitation Learning from Imperfect Demonstration. In *Proceedings of the Thirty-Sixth International Conference on Machine Learning*, Proceedings of Machine Learning Research, 6818–6827. Long Beach, CA, USA: PMLR.
- Yu, T.; Thomas, G.; Yu, L.; Ermon, S.; Zou, J. Y.; Levine, S.; Finn, C.; and Ma, T. 2020. MOPO: Model-based Offline Policy Optimization. In *Advances in Neural Informa-*

*tion Processing Systems*, volume 33, 14129–14142. Virtual: Curran Associates, Inc.

Zhan, X.; Zhu, X.; and Xu, H. 2022. Model-Based Offline Planning with Trajectory Pruning. In *Proceedings of the Thirty-First International Joint Conference on Artificial Intelligence*, 3716–3722. International Joint Conferences on Artificial Intelligence Organization.

Zhang, H.; Shao, J.; Jiang, Y.; He, S.; Zhang, G.; and Ji, X. 2022. State Deviation Correction for Offline Reinforcement Learning. In *Proceedings of the Thirty-Sixth AAAI Conference on Artificial Intelligence*, 9022–9030. Virtual: AAAI Press.

Zhou, W.; Bajracharya, S.; and Held, D. 2020. PLAS: Latent Action Space for Offline Reinforcement Learning. In *Proceedings of the Fourth Conference on Robot Learning*, 1719–1735. Virtual: PMLR.

## A Details for the Proposed Methods

This section presents details of the proposed model, the proposed learning algorithm and LBRAC-v.

Except for  $K$ , this work uses same values of hyper-parameters on all datasets. The dimensionality of embedding spaces ( $d_e$ ) is set to eight.  $f_s$  is parameterized with two layers of feedforward networks whose hidden dimension and output dimension are 200 ( $d_\phi = 200$ ). The output of  $f_s$  is processed with the layer norm operation (Ba, Kiros, and Hinton 2016).  $f_p$  is parameterized with two layers of feed-forward networks with 200 as hidden dimension and  $2 \times d_A$  as output dimension.  $f_Q$  and  $f_{s,a}$  are parameterized similarly but with  $d'_\phi = 300$ . This work uses the Relu function as the activation function for all hidden layers and output of  $f_s$  and  $f_{s,a}$ .

The output of  $f_p$  parameterizes an action distribution as follows.  $f_p$  uses the location-scale reparameterization to compute Gaussian action distributions using  $\mathcal{N}(0, I_{d_A})$ , where  $I_{d_A}$  means an identity matrix in  $\mathbb{R}^{d_A}$ . The mean part of action distribution,  $\mu_s$ , is first squashed into  $[-1, 1]$  using the  $\tanh(\cdot)$  function and then mapped to the range of actions via affine transformation.  $f_p$  in fact outputs  $\log(\sigma_s)$  instead of  $\sigma_s$  directly, which is clipped to  $[-10, 10]$  before passing to the exponential function. Then a multi-variate Gaussian distribution for actions can be obtained with  $\mu_s$  and  $\sigma_s$ .

Meanwhile, similar to BRAC-v, the present study utilizes an ensemble of two functions for the Q network part. Each of them contains a set of  $f_{s,a}$ ,  $H$  and  $f_Q$ .

Algorithm 1 presents pseudocode for learning the proposed model. This work uses  $5 \times 10^{-5}$  as the learning rate for  $f_s$ ,  $f_p$ ,  $W$  and  $E$ . For  $f_{s,a}$ ,  $H$  and  $f_Q$ , the learning rate is set to  $1 \times 10^{-4}$ . The rate of soft update for target networks is 0.001. Rows of  $E$ ,  $W$ , and  $H$  are normalized by  $l_2$ -norm.

Algorithm 2 presents pseudocode for the proposed LBRAC-v. All of the hyper-parameters are the same with the learning algorithm for the proposed model. Before policy learning,  $e_\pi$  and  $h_\pi$  is initialized with the vector of the best policy in  $\mathcal{B}$  and its Q-function. The best policy is determined as follows. First compute the percentiles  $\{q_i\}$  of trajectories returns and use them to discretize returns. In other words, the discretized return of  $\tau_m, g_m$ , is  $j$  if  $q_j \leq \sum_t r_{m,t} < q_{j+1}$ , where  $q_j$  and  $q_{j+1}$  are two consecutive percentile values such as 95 and 96. This quantization is employed to improve the robustness against extreme values. Then for each  $b_k \in \mathcal{B}$ , compute the average of discretized returns of the trajectories assigned to it. The one with the largest average discretized return is considered as the best behavior policy.

## B Details for Experiments

### Details for heterogeneous- $k$ Datasets

The proposed heterogeneous- $k$  datasets are generated in a similar way as the medium versions in the D4RL benchmark. The behavior policies are trained using the SAC algorithm implemented in rllkit repository<sup>3</sup>. As in practice dataset provided to offline policy learners are rarely of superior quality, the behavior policies are trained from scratch

<sup>3</sup><https://github.com/rail-berkeley/rllkit>

---

### Algorithm 1: Learning the proposed model

---

**Input:**  $D = \{(s_m, a_m, r_m, s'_m)\}_{m=1}^M$   
 $T$ , the number of training steps  
**Output:**  $\{b_k\}_{k=1}^K$  and  $\{Q^{b_k}\}_{k=1}^K$   
Initialize  $f_s, f_p, f_{s,a}, f_Q, W, E$  and  $H$ .  
**for**  $t = 1, 2, \dots, T$  **do**  
    Sample a batch of transitions  $D_{\text{batch}}$  from  $D$ .  
    Look up  $w_m$  for transitions in  $D_{\text{batch}}$  and  
    normalize them by  $l_2$  norm.  
    Normalize rows of  $E$  by  $l_2$  norm, and compute  
     $\tilde{z}_m = \arg\max_j e_j w_m$  for  $w_m$  of  $D_{\text{batch}}$   
    Update  $f_s, f_p, W$  and  $E$  by minimizing  
     $L_{\text{rec}} + \alpha L_{\text{com}}$ .  
    Normalize rows of  $H$  by  $l_2$  norm, and update  
     $f_{s,a}, f_Q, H$  by minimizing  $L_Q$ .  
**end**

---

for only one million gradient steps, while by default SAC agents are trained for three million gradient steps. The five behavior policies for a task are trained with random seeds one to five. Table 2 shows the normalized returns of these behavior policies.

For each task, the heterogeneous- $k$  dataset is generated by rolling out the first  $k$  policies using the code provided by Fu et al. (2020). Each policy generates an even amount of transitions. Following the standard of these tasks, a trajectory starts after resetting the environment, and it ends if a terminal signal is received, or the number of steps reaches 1000. Statistics of these datasets can be found in Table 3.

### Details for Other Datasets

Datasets other than the heterogeneous- $k$  are released by Fu et al. (2020). As shown in Table 3, for the same tasks they differ in behavior policies, size, trajectory returns and number of transitions. In particular, Figure 8 shows the distribution of return for the medium-replay versions. It shows that the return distribution for halfcheetah appears to be bi-modal, containing many high-return trajectories. In contrast, most of the trajectories in this version for walker2d and hopper are low-return trajectories.

### Return Normalization

Throughout this paper, trajectory returns are normalized as suggested by Fu et al. (2020). The test returns of an algorithm obtained for some task is transformed using the equation  $100 * \frac{\text{return} - \text{random return}}{\text{expert return} - \text{random return}}$ . This transformation eliminates the range difference in returns and makes results more comprehensible. Values of random returns and expert returns are taken from (Fu et al. 2020). In specific, the return for a random policy on halfcheetah, walker2d and hopper are -280.18, 1.63 and -20.27, respectively. The return for expert demonstrations on these tasks are 12135.0, 4592.3, and 3234.3.



**Algorithm 2: LBRAC-v**

**Input:**  $D = \{(s_m, a_m, r_m, s'_m)\}_{m=1}^M$ ,  
 $T$ , the number of training steps  
Trained  $f_s, f_p, f_{s,a}, f_Q, W, E$  and  $H$ .  
**Output:**  $\pi$   
Compute the percentiles  $\{q_j\}_{j=0}^{99}$  of  $\{\sum_t r_{m,t}\}_{m=1}^M$ .  
Compute the discretized returns  $g_m$ .  $g_m = j$  if  
 $q_j \leq \sum_t r_{m,t} < q_{j+1}$ .  
For each  $b_k$ , compute  $u_k = \frac{\sum_{m=1}^M G_{k,m} * \bar{g}_m}{\sum_{m=1}^M G_{k,m}}$   
Let  $k^* = \operatorname{argmax}_k u_k$ , and initialize  $e_\pi$  as  $e_{k^*}$  and  
the  $h_\pi$  as  $h_{k^*}$ .  
**for**  $t = 1, 2, \dots, T$  **do**  
    Sample a batch of transitions  $D_{\text{batch}}$  from  $D$ .  
    Look up  $w_m$  for transitions in  $D_{\text{batch}}$  and  
    normalize them by  $\ell_2$  norm.  
    Normalize rows of  $E$  by  $\ell_2$  norm, and compute  
     $\tilde{z}_m = \operatorname{argmax}_j e_j w_m$  for  $w_m$  of  $D_{\text{batch}}$   
    Update  $f_s, f_p, W, E$  and  $e_\pi$  by minimizing  
     $L_{\text{rec}} + \alpha L_{\text{com}} + L_{\text{actor}}$ .  
    Normalize rows of  $H$  by  $\ell_2$  norm, and update  
     $f_{s,a}, f_Q, H$  and  $h_\pi$  by minimizing  $L_Q + L_{\text{critic}}$ .  
**end**

Table 2: Normalized returns of behavior policies of heterogeneous- $k$  datasets.

	1 <sup>st</sup> policy	2 <sup>nd</sup> policy	3 <sup>rd</sup> policy	4 <sup>th</sup> policy	5 <sup>th</sup> policy
halfcheetah	72.75	81.90	84.78	84.92	66.86
waker2d	88.43	103.84	85.32	100.91	83.10
hopper	108.57	106.03	99.69	79.87	85.33

**Details for Alternative Methods**

For D4RL datasets, results of BRAC-v, CQL and BCQ are taken from (Fu et al. 2020), and results of PLAS and MOPO are taken from their original paper. For the proposed datasets, the present study runs the code provided by Fu et al. (2020) for BRAC-v and BCQ, the code released in their original papers for CQL, PLAS and MOPO. However, some modifications is required for adapt the code for CQL for the latest version of PyTorch platform.

Following the methodology of Fu et al. (2020), algorithms are trained for 0.5 million gradient steps. For other, the present study sticks with the value suggested in the corresponding code base or papers.

**C Additional Results****Discussion for Medium-Replay Datasets**

In Table 1, on the medium-replay version of halfcheetah BRAC-v and CQL do not perform as poor as they are on the medium-replay version of other two tasks. This works explain such observation with the distribution of trajectory returns in these datasets. As shown in Table 3, the normalized return of the medium-replay version for halfcheetah is much higher than the medium replay versions for walker2d

Table 3: Statistics of datasets. The random, medium, medium-replay, and medium-expert versions are provided by Fu et al. (2020). The heterogeneous- $k$  ( $k \in \{1, 2, 3, 4, 5\}$ ) versions are proposed by the present study. The return column shows the average of normalized trajectory return in a dataset.

Task	Version	M	#transitions	Normalized Return
halfcheetah	random	1000	1000000	-0.26
	medium	1000	1000000	155.8
	medium-replay	202	202000	103.65
	medium-expert	2000	2000000	245.61
	heterogeneous-1	1000	1000000	69.91
	heterogeneous-2	1000	1000000	73.91
	heterogeneous-3	1000	1000000	76.14
	heterogeneous-4	1000	1000000	77.47
	heterogeneous-5	1000	1000000	74.76
walker2d	random	48907	1000000	0.01
	medium	513	1000000	202.84
	medium-replay	791	302000	28.90
	medium-expert	514	1999995	496.24
	heterogeneous-1	1037	1000000	88.79
	heterogeneous-2	1015	1000000	88.62
	heterogeneous-3	1018	1000000	85.93
	heterogeneous-4	1006	1000000	92.33
	heterogeneous-5	1018	1000000	92.29
hopper	random	45239	1000000	1.19
	medium	2185	1000000	44.32
	medium-replay	1639	402000	18.49
	medium-expert	2274	1999906	91.33
	heterogeneous-1	1180	1000000	94.72
	heterogeneous-2	1207	1000000	93.23
	heterogeneous-3	1454	1000000	76.67
	heterogeneous-4	1513	1000000	73.08
	heterogeneous-5	1695	1000000	65.88

and hopper. Moreover, as shown in Figure 8, the medium-replay versions of walker2d and hopper are dominated by poor trajectories. The same version for halfcheetah, on the contrary, has much more good trajectories. As this version contains trajectories collected during training a RL agent, this indicates a faster convergence on halfcheetah than on other task. In consequence, this version for halfcheetah are generated by less policies than the same version for other tasks.

**Results for Varying  $K$** 

Table 4 shows the results of LBRAC-v for different  $K$  on the D4RL datasets. The best value of  $K$  is dataset dependent. For example, the best value for the medium version of halfcheetah is  $K = 5$ , but for the random version it is  $K = 15$ .

**Additional Visualizations**

Figure 9a, Figure 9b, Figure 9c and Figure 9d presents visualizations obtained during training the proposed model and LBRAC-v for  $K = 1$  and  $K = 10$ .

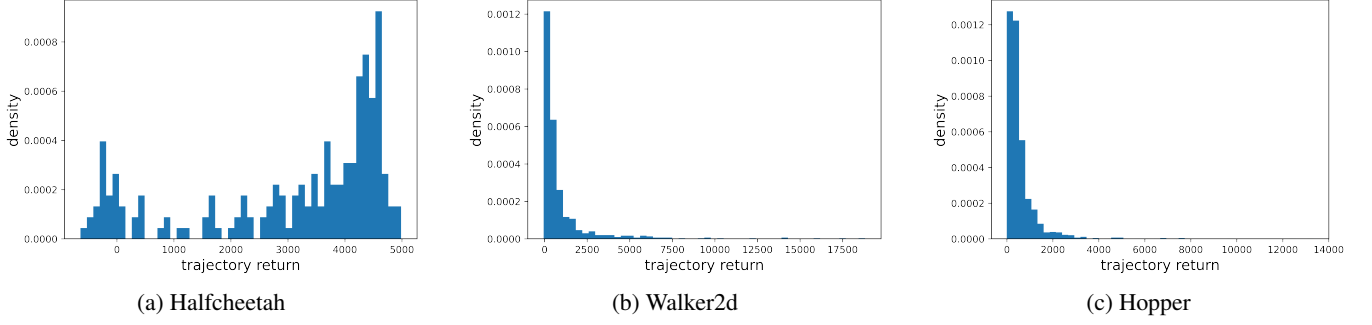


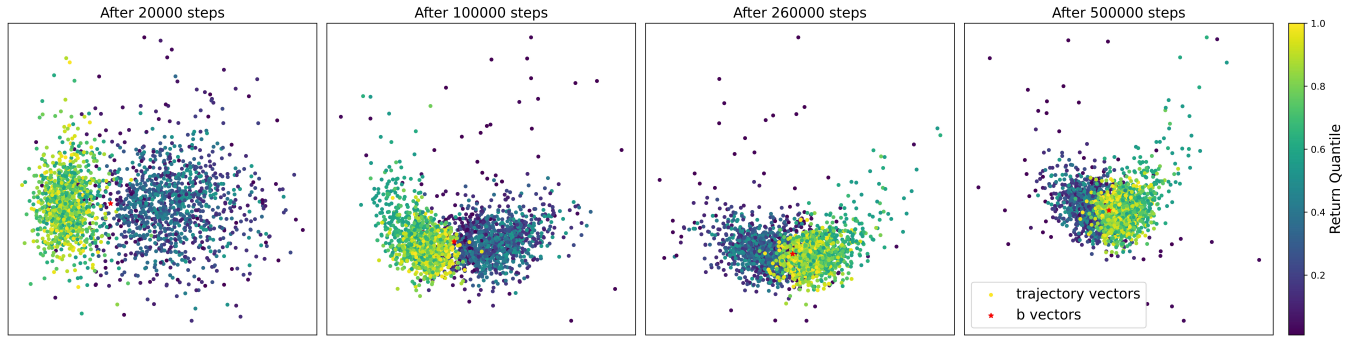
Figure 8: Histogram of trajectory returns for the medium-replay versions of the three tasks. Unlike the medium-replay versions for hopper and walker2d, this version for halfcheetah is not dominated by poor trajectories.

Table 4: Normalized return of LBRAC-v for different  $K$  on the D4RL datasets. The best value for  $K$  is dataset-dependent.

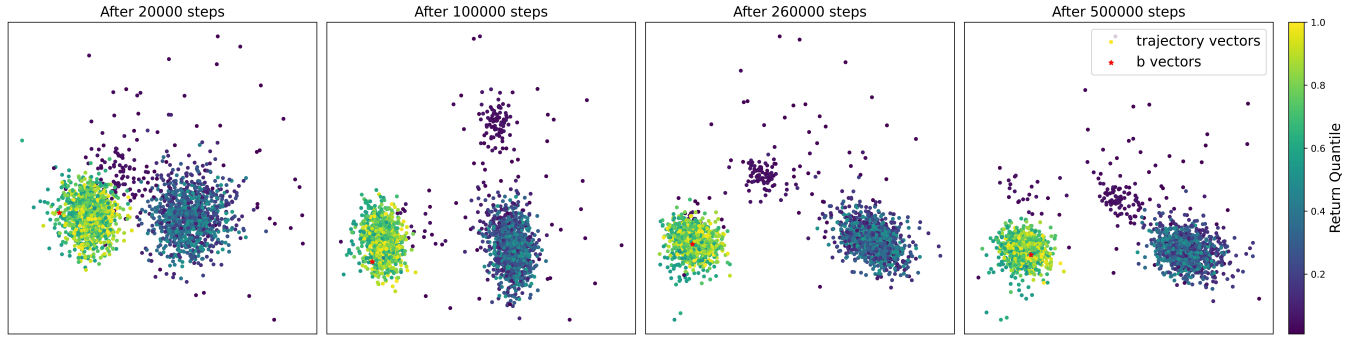
Task	Version	$K=1$	$K=5$	$K=10$	$K=15$	$K=20$
halfcheetah	random	$25.75 \pm 0.38$	$25.55 \pm 0.24$	$25.01 \pm 0.39$	<b><math>26.37 \pm 0.29</math></b>	$25.44 \pm 0.23$
	medium	$51.93 \pm 0.13$	<b><math>52.14 \pm 0.11</math></b>	$51.71 \pm 0.11$	$52.01 \pm 0.11$	$51.56 \pm 0.17$
	medium-replay	<b><math>48.41 \pm 0.14</math></b>	$48.16 \pm 0.18$	$47.94 \pm 0.12$	$47.99 \pm 0.17$	$47.89 \pm 0.09$
	medium-expert	$93.14 \pm 1.05$	$91.54 \pm 1.36$	$91.22 \pm 1.15$	<b><math>94.22 \pm 1.00</math></b>	$92.44 \pm 1.26$
walker2d	random	<b><math>11.96 \pm 4.39</math></b>	$10.22 \pm 2.56$	$7.10 \pm 1.75$	$8.53 \pm 3.15$	$10.82 \pm 4.18$
	medium	$77.98 \pm 1.74$	$80.56 \pm 1.45$	$78.45 \pm 2.27$	$79.63 \pm 2.17$	<b><math>82.40 \pm 1.30</math></b>
	medium-replay	$61.93 \pm 5.08$	$65.53 \pm 3.45$	$63.79 \pm 4.21$	$74.20 \pm 3.74$	<b><math>76.18 \pm 4.47</math></b>
	medium-expert	$109.52 \pm 0.25$	$109.37 \pm 0.16$	$109.36 \pm 0.20$	$109.57 \pm 0.26$	<b><math>109.65 \pm 0.23</math></b>
hopper	random	$9.43 \pm 0.49$	$8.96 \pm 0.32$	$8.75 \pm 0.66$	<b><math>9.63 \pm 0.27</math></b>	$8.46 \pm 0.16$
	medium	$97.73 \pm 2.56$	$96.46 \pm 1.52$	$100.20 \pm 1.03$	<b><math>100.50 \pm 0.57</math></b>	$96.16 \pm 2.52$
	medium-replay	<b><math>81.89 \pm 12.77</math></b>	$47.69 \pm 10.17$	$78.45 \pm 12.67$	$78.37 \pm 10.66$	$64.94 \pm 9.17$
	medium-expert	$82.06 \pm 14.33$	$73.27 \pm 13.50$	$82.07 \pm 11.69$	$76.92 \pm 7.84$	<b><math>98.08 \pm 6.39</math></b>

Table 5: Relative return of LBRAC-v and for different  $K$  on the heterogeneous- $k$  datasets.

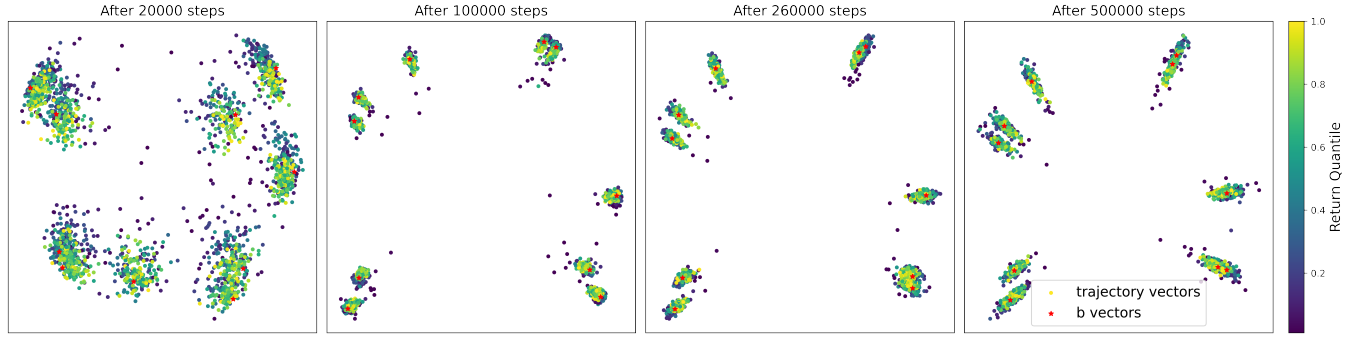
Task	#Behavior Policy	$K=1$	$K=5$	$K=10$	$K=15$	$K=20$
halfcheetah	1	$1.0129 \pm 0.0073$	$0.9988 \pm 0.0056$	<b><math>1.0244 \pm 0.0025</math></b>	$1.0056 \pm 0.0078$	$0.9922 \pm 0.0164$
	2	<b><math>1.0106 \pm 0.0118</math></b>	$0.9686 \pm 0.0229$	$0.9914 \pm 0.0286$	$0.9741 \pm 0.0269$	$0.9707 \pm 0.0125$
	3	$0.9160 \pm 0.0369$	$0.8757 \pm 0.0738$	$0.9608 \pm 0.0114$	$0.9578 \pm 0.0311$	<b><math>0.9709 \pm 0.0450</math></b>
	4	$0.9035 \pm 0.0424$	$0.9574 \pm 0.0124$	$0.9643 \pm 0.0249$	$0.9616 \pm 0.0202$	<b><math>0.9761 \pm 0.0178</math></b>
	5	$0.8754 \pm 0.0394$	$0.8632 \pm 0.0371$	<b><math>0.8856 \pm 0.0237</math></b>	$0.8666 \pm 0.0473$	$0.5129 \pm 0.0448$
walker2d	1	$1.0422 \pm 0.0094$	<b><math>1.0556 \pm 0.0044</math></b>	$1.0524 \pm 0.0026$	$1.0513 \pm 0.0032$	$1.0510 \pm 0.0016$
	2	$1.0250 \pm 0.0187$	$0.9560 \pm 0.0566$	<b><math>1.0392 \pm 0.0183</math></b>	$1.0060 \pm 0.0079$	$1.0371 \pm 0.0205$
	3	$0.7741 \pm 0.1871$	<b><math>0.8779 \pm 0.1516</math></b>	$0.7664 \pm 0.1224$	$0.6280 \pm 0.1160$	$0.5828 \pm 0.1943$
	4	<b><math>0.9442 \pm 0.0355</math></b>	$0.8178 \pm 0.0680$	$0.8268 \pm 0.1004$	$0.7786 \pm 0.1298$	$0.7642 \pm 0.0965$
	5	<b><math>1.0113 \pm 0.0389</math></b>	$0.8073 \pm 0.1039$	$0.8709 \pm 0.1251$	$0.9192 \pm 0.0784$	$0.8308 \pm 0.1683$
hopper	1	$0.9052 \pm 0.0315$	$0.9237 \pm 0.0217$	$0.9352 \pm 0.0338$	$0.9355 \pm 0.0186$	<b><math>0.9618 \pm 0.0147</math></b>
	2	$0.9650 \pm 0.0364$	$0.9101 \pm 0.0504$	$0.9472 \pm 0.0590$	<b><math>0.9914 \pm 0.0197</math></b>	$0.9477 \pm 0.0445$
	3	$1.0614 \pm 0.0099$	$1.0535 \pm 0.0142$	$1.0630 \pm 0.0080$	<b><math>1.0669 \pm 0.0050</math></b>	$1.0654 \pm 0.0101$
	4	$1.0710 \pm 0.0451$	$1.0129 \pm 0.0447$	$1.1072 \pm 0.0133$	$0.9505 \pm 0.0949$	<b><math>1.1168 \pm 0.0128</math></b>
	5	$1.0738 \pm 0.0508$	$1.0044 \pm 0.0354$	<b><math>1.1354 \pm 0.0146</math></b>	$0.9162 \pm 0.1295$	$0.9500 \pm 0.0947$



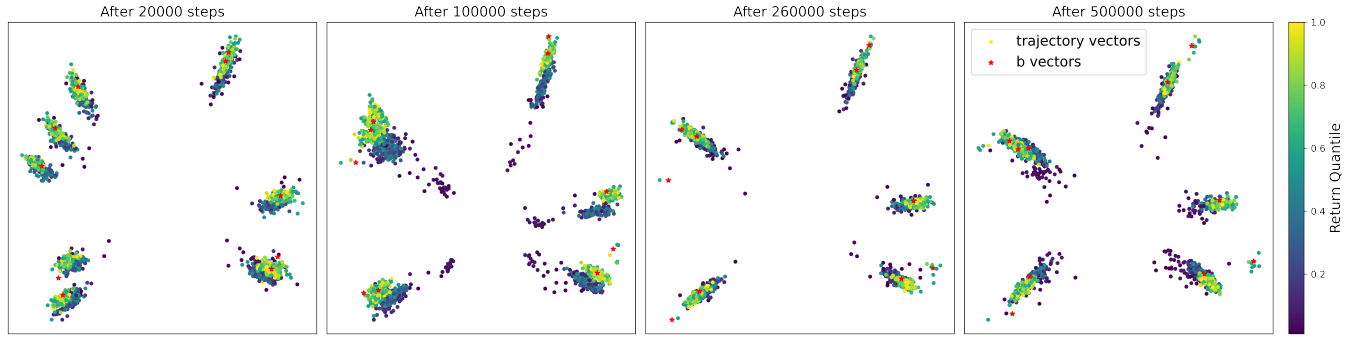
(a) The proposed model for  $K = 1$ .



(b) LBRAC-v for  $K = 1$ .



(c) The proposed model for  $K = 10$ .



(d) LBRAC-v for  $K = 10$ .

Figure 9: Visualizations for the proposed model and LBRAC-v during training.